Asian Journal of Chemistry; Vol. 37, No. 3 (2025), 521-528

ASIAN JOURNAL OF CHEMISTRY

https://doi.org/10.14233/ajchem.2025.33158

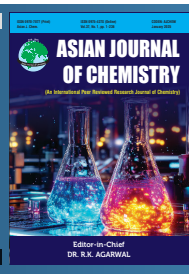

Design, Synthesis and Anticancer Activity of Benzothiazole Hybrids: Insights from Molecular Docking Studies

RAJU KOTTE[1,2,*] and GIRIJA SASTRY VEDULA[1]

[1]AU College of Pharmaceutical Sciences, Andhra University, Visakhapatnam-530003, India
[2]Sir C.R. Reddy College of Pharmaceutical Sciences, Affiliated to Andhra University, Eluru-534007, India

*Corresponding author: E-mail: jnvraju@gmail.com

Received: 23 December 2024; *Accepted*: 21 January 2025; *Published online*: 28 February 2025; AJC-21906

A series of benzothiazole hybrids **5a-n** bearing acetamide and benzamide functionalities were synthesized and evaluated for their anticancer activity and binding affinity with epidermal growth factor receptor (EGFR) targets, 4WKQ and 6LUD. The synthesis involved the synthesis of 6-hydroxy-2-aminobenzothiazole, followed by methylation and coupling with carboxylic acids to yield benzothiazole hybrid compounds. The structures of the synthesized compounds were confirmed using analytical techniques such as ^{1}H NMR, ^{13}C NMR and HRMS techniques. Molecular docking studies indicated that the hydroxyl (-OH) and amino (-NH_2) groups significantly enhanced binding to both EGFR targets, with compounds **5j** (3-OH) and **5i** (4-OH) showing the highest binding affinities. The anticancer activity of these hybrids was tested against MCF-7 breast cancer, HCT-116 colon cancer and HEK-293 normal cells using MTT assays. The compounds exhibited promising cytotoxicity, with *meta*-substituted derivatives showing superior activity. Among them, compounds **5f**, **5h**, **5i**, **5j** and **5m** demonstrated a significant potency, suggesting their potential as candidates for further development in cancer research.

Keywords: Benzothiazoles, Anticancer activity, Molecular docking, EGFR inhibitors, MCF-7, HCT-116.

INTRODUCTION

Cancer continues to be one of the most pressing global health challenges, characterized by an increasing incidence rate and placing a significant strain on healthcare systems worldwide [1]. This disease encompasses a broad spectrum of malignancies, each with distinct biological complexities that make its treatment particularly challenging. Despite the substantial progress achieved in the development of diagnostic techniques and therapeutic strategies including surgery, radiation and chemotherapeutic agents, several barriers persist in achieving optimal patient outcomes. Among these, the development of drug resistance whether intrinsic or acquired poses a significant hurdle, often leading to treatment failure and disease progression [2,3]. Furthermore, the intricate biology of cancer, marked by genetic heterogeneity, dysregulated signalling pathways and an evolving tumour microenvironment, underscores the necessity for innovative approaches to combat this disease effectively.

To address these challenges, there is an urgent need for the discovery and development of novel anticancer agents that can selectively target key molecular pathways critical to tumour initiation, growth and metastasis. Such selective targeting holds promise not only for enhancing the therapeutic efficacy of anticancer agents but also for minimizing off-target effects and associated toxicities, thereby improving patient quality of life. The pursuit of these new compounds is rooted in advancing the understanding of cancer biology, integrating emerging technologies such as high-throughput screening, molecular docking and structure-based drug design and leveraging the potential of synthetic and natural product-based chemistries [4].

Benzothiazole scaffolds have garnered significant attention in drug discovery due to their ease of synthesis [5,6] and broad spectrum of therapeutic activities [7,8]. Within this class, 2-substituted benzothiazoles such as amino benzothiazole [9-12], mercapto benzothiazole [13-17] and aryl benzothiazole [18-20] have exhibited remarkable anticancer activity across various *in vitro* and *in vivo* cancer models. The therapeutic potential of benzothiazole derivatives is exemplified by compounds like riluzole, which are currently undergoing clinical trials, further validating their promise as chemotherapeutic agents [21,22].

Recent studies have highlighted the efficacy of 2-substituted benzothiazoles in targeting the epidermal growth factor receptor (EGFR), a pivotal protein regulating cell proliferation and survival. Evidence suggests that these derivatives can effectively inhibit EGFR signaling pathways, a mechanism critical in cancers characterized by EGFR overexpression or mutations [23-26]. These findings emphasize the potential of 2-substituted benzothiazoles as potent EGFR inhibitors, underscoring their relevance and promise in the development of targeted therapies for cancer treatment.

The study encompasses the systematic synthesis of these hybrids and their comprehensive evaluation for anticancer activity against established cancer cell lines, including MCF-7 (breast cancer) and HCT-116 (colon cancer), alongside a normal human cell line (HEK-293) to assess selectivity. The novelty of the present work lies in its integration of synthetic chemistry with advanced molecular docking studies, emphasizing the binding interactions of the synthesized hybrids with EGFR. Docking studies utilize high-resolution crystal structures of EGFR in complex with the clinically relevant inhibitors gefitinib (PDB ID: 4WKQ) and osimertinib (PDB ID: 6LUD) to elucidate the binding modes and affinities. By combining experimental synthesis with *in silico* approaches, this research aims to identify promising lead compounds with enhanced anticancer efficacy and selectivity, offering potential advancements in the development of targeted therapies for breast and colon cancers.

EXPERIMENTAL

Synthetic-grade chemicals and solvents were sourced from Sigma-Aldrich, Bangalore, India and used without further purification. Reactions were monitored using Merck-precoated aluminium TLC plates with silica gel 60 F_{254}. The melting points were determined with a Remi electronic melting point apparatus. ^{1}H and ^{13}C NMR spectra were recorded using a BRUKER DRX spectrometer, with tetramethyl silane as the internal reference for chemical shift calibration in ppm. High-resolution mass spectrometry (HRMS) spectra were obtained in positive ionization mode using a Waters Xevo Q-Tof mass spectrometer. A-549, PANC-1 and HEK-293 cell lines were acquired from ATCC and procured through Himedia Pvt. Ltd., India.

Synthesis of 2-aminobenzo[*d*]thiazol-6-ol (3): The synthesis of 6-hydroxy-2-aminobenzothiazole (**3**) began with the condensation reaction between benzoquinone and thiourea in refluxing ethanol, catalyzed by a small amount of conc. HCl. The reaction was conducted under reflux conditions, ensuring thorough mixing and efficient progress of the reaction. Using an appropriate solvent solution and TLC analysis, the progress of the reaction could be monitored. After completion, the reaction mixture was allowed to cool and the product was extracted with ethyl acetate or dichloromethane. The organic layer was then washed with water to remove impurities, followed by drying over anhydrousNs_2SO_4. Concentration of the solvent under reduced pressure yielded the crude product, which was further purified through recrystallization with ethanol. The resulting pure compound, 6-hydroxy-2-aminobenzothiazole (**3**), was obtained after filtration and vacuum drying [27].

Synthesis of 6-methoxybenzo[*d*]thiazol-2-amine (4): To a solution of 2-aminobenzo[*d*]thiazol-6-ol (**3**) (1 equiv.) in DMF (5 mL), K_2CO_3 (2.5 equiv.) and CH_3I (1.1 equiv. for **1a**) was added. The mixture was stirred at room temperature overnight. The solvent was evaporated under reduced pressure and the residue was suspended in AcOEt and washed with saturated of K_2CO_3 solution and brine. The organic phase was dried over Na_2SO_4 and concentrated. The crude was chromatographed on silica gel to afford the desired product [27].

General procedure for the synthesis of benzothiazole hybrids (5a-n): To a stirred solution of substituted carboxylic acid (1 mmol) in aqueous medium was added N,N′-diisopropylcarbodiimide (1 mmol) and the reaction mixture was stirred at room temperature for 1 h. After this period, amine (1 mmol) was added and the reaction mixture was stirred at room temperature for the indicated time until the starting materials were totally consumed as checked by TLC (**Scheme-I**). Then, the solvent was separated by filtration and the solid washed several times with lukewarm water in order to remove the byproduct diisopropyl urea (DIU) [28].

***N*-(6-Methoxybenzo[*d*]thiazol-2-yl)acetamide (5a):** White solid, yield 83%, m.p.: 158-159 ºC; ^{1}H NMR (500 MHz, chloroform-d_6) δ ppm: 10.94 (s, 1H), 7.56 (d, J = 7.8 Hz, 1H), 7.47 (d, J = 2.3 Hz, 1H), 7.13 (dd, J = 7.6, 2.2 Hz, 1H), 3.72 (s, 3H), 2.31 (s, 3H). ^{13}C NMR (125 MHz, chloroform-d_6) δ ppm: 169.59, 159.01, 154.88, 145.28, 131.59, 118.80, 113.30, 105.52, 54.98, 21.19. HRMS: *m/z* for $C_{10}H_{10}N_2O_2S$ ($[M + H]^+$): 223.0548, found 223.0545.

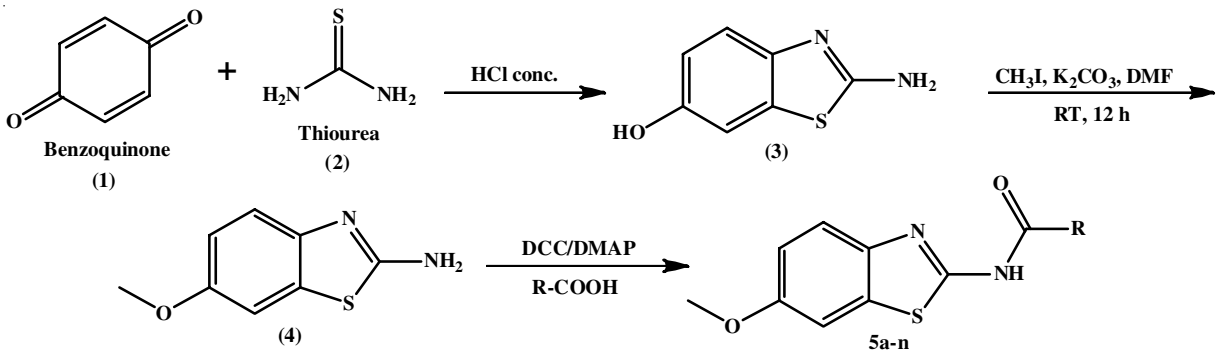

R = -CH_3, -CH_2-CH_3, -CH_2-CH_2-CH_3, -C_6H_5, -(C_6H_4)-4-CH_3, -(C_6H_4)-3-CH_3, -(C_6H_4)-4-Cl, -(C_6H_4)-3-Cl, -(C_6H_4)-4-OH, -(C_6H_4)-3-OH, -(C_6H_4)-4-NO_2, -(C_6H_4)-3-NO_2, -(C_6H_4)-4-NH_2, -(C_6H_4)-4-COOH

Scheme-I: Scheme of synthesis for benzothiazole carboxamide hybrids

***N*-(6-Methoxybenzo[*d*]thiazol-2-yl)propionamide (5b):** White solid, yield 80%, m.p.: 145-146 ºC; ^{1}H NMR (500 MHz, chloroform-d_6) δ ppm: 10.92 (s, 1H), 7.64 (d, *J* = 7.8 Hz, 1H), 7.53 (d, *J* = 2.1 Hz, 1H), 7.06 (dd, *J* = 7.7, 2.2 Hz, 1H), 3.74 (s, 3H), 2.51 (q, *J* = 7.1 Hz, 2H), 1.22 (t, *J* = 7.1 Hz, 3H). ^{13}C NMR (125 MHz, chloroform-d_6) δ ppm: 171.99, 159.72, 153.63, 144.64, 130.79, 118.25, 112.38, 106.73, 54.47, 28.37, 11.63. HRMS: *m/z* for $C_{11}H_{12}N_2O_2S$ ([M + H]$^+$): 237.0716, found 237.0712.

***N*-(6-Methoxybenzo[*d*]thiazol-2-yl)butyramide (5c):** White solid, yield 76%, m.p.: 151-152 ºC; ^{1}H NMR (500 MHz, chloroform-d_6) δ ppm: 10.87 (s, 1H), 7.59 (d, *J* = 7.8 Hz, 1H), 7.44 (d, *J* = 2.2 Hz, 1H), 6.99 (dd, *J* = 7.8, 2.1 Hz, 1H), 3.71 (s, 3H), 2.43 (t, *J* = 6.2 Hz, 2H), 1.68 (dtd, *J* = 13.8, 7.6, 6.1 Hz, 2H), 1.05 (t, *J* = 7.6 Hz, 3H). ^{13}C NMR (125 MHz, chloroform-d_6) δ ppm: 173.36, 159.93, 155.73, 146.31, 130.79, 119.70, 112.38, 104.63, 56.13, 37.07, 18.23, 12.35. HRMS: *m/z* for $C_{12}H_{14}N_2O_2S$ ([M + H]$^+$): 251.0795, found 251.0790.

***N*-(6-Methoxybenzo[*d*]thiazol-2-yl)benzamide (5d):** White solid, yield 87%, m.p.: 194-195 ºC; ^{1}H NMR (500 MHz, chloroform-d_6) δ ppm: 10.97 (s, 1H), 8.00-7.93 (m, 2H), 7.59 (d, *J* = 7.8 Hz, 1H), 7.51 (d, *J* = 2.0 Hz, 1H), 7.43-7.36 (m, 1H), 7.33-7.27 (m, 2H), 7.01 (dd, *J* = 7.7, 2.2 Hz, 1H), 3.74 (s, 3H). ^{13}C NMR (125 MHz, chloroform-d_6) δ ppm: 168.20, 158.56, 154.06, 144.64, 132.68, 131.69, 130.50, 127.97, 126.08, 119.70, 114.27, 110.50, 53.52. HRMS: *m/z* for $C_{15}H_{12}N_2O_2S$ ([M + H]$^+$): 285.0681, found 285.0678.

***N*-(6-Methoxybenzo[*d*]thiazol-2-yl)-4-methylbenzamide (5e):** White solid, yield 81%, m.p.: 188-189 ºC; ^{1}H NMR (500 MHz, chloroform-d_6) δ ppm: 10.98 (s, 1H), 7.68 (d, *J* = 8.0 Hz, 2H), 7.53 (d, *J* = 7.7 Hz, 1H), 7.45 (d, *J* = 2.1 Hz, 1H), 7.24 (d, *J* = 8.0 Hz, 2H), 7.01 (dd, *J* = 7.7, 2.2 Hz, 1H), 3.71 (s, 3H), 2.26 (s, 3H). ^{13}C NMR (125 MHz, chloroform-d_6) δ ppm: 168.94, 160.44, 154.06, 146.31, 140.14, 132.90, 131.95, 129.34, 127.97, 118.04, 114.05, 110.28, 53.74, 21.99. HRMS: *m/z* for $C_{16}H_{14}N_2O_2S$ ([M + H]$^+$): 299.0796, found 299.0796.

***N*-(6-Methoxybenzo[*d*]thiazol-2-yl)-3-methylbenzamide (5f):** White solid, yield 76%, m.p.: 183-184 ºC; ^{1}H NMR (500 MHz, chloroform-d_6) δ ppm: 10.91 (s, 1H), 7.82 (dd, *J* = 7.3, 1.5 Hz, 2H), 7.59 (d, *J* = 7.8 Hz, 1H), 7.51 (d, *J* = 2.1 Hz, 1H), 7.39 (t, *J* = 7.7 Hz, 1H), 7.30 (dt, *J* = 7.3, 1.9 Hz, 1H), 7.01 (dd, *J* = 7.7, 2.2 Hz, 1H), 3.77 (s, 3H), 2.36 (s, 3H). ^{13}C NMR (125 MHz, chloroform-d_6) δ ppm: 168.41, 158.56, 153.85, 144.20, 136.88, 133.84, 131.69, 130.85, 128.48, 128.02, 125.62, 119.70, 114.77, 109.77, 54.25, 22.00. HRMS: *m/z* for $C_{16}H_{14}N_2O_2S$ ([M + H]$^+$): 299.0795, found 299.0791.

4-Chloro-*N*-(6-methoxybenzo[*d*]thiazol-2-yl)benzamide (5g): White solid, yield 80%, m.p.: 208-209 ºC; ^{1}H NMR (500 MHz, chloroform-d_6) δ ppm: 10.94 (s, 1H), 7.76 (d, *J* = 8.3 Hz, 2H), 7.59 (d, *J* = 7.8 Hz, 1H), 7.45 (d, *J* = 2.2 Hz, 1H), 7.40-7.34 (m, 2H), 7.10 (dd, *J* = 7.8, 2.1 Hz, 1H), 3.81 (s, 3H). ^{13}C NMR (125 MHz, chloroform-d_6) δ ppm: 167.98, 160.44, 154.28, 144.86, 136.88, 132.68, 131.95, 129.61, 128.40, 118.25, 114.05, 109.34, 54.04. HRMS: *m/z* for $C_{15}H_{11}ClN_2O_2S$ ([M + H]$^+$): 320.0207, found 320.0205.

3-Chloro-*N*-(6-methoxybenzo[*d*]thiazol-2-yl)benzamide (5h): White solid, yield 77%, m.p.: 205-206 ºC; ^{1}H NMR (500 MHz, chloroform-d_6) δ ppm: 10.94 (s, 1H), 7.87 (t, *J* = 2.2 Hz, 1H), 7.79-7.73 (m, 1H), 7.56 (d, *J* = 7.8 Hz, 1H), 7.50 (t, *J* = 8.0 Hz, 1H), 7.45-7.37 (m, 2H), 7.04 (dd, *J* = 7.7, 2.2 Hz, 1H), 3.75 (s, 3H). ^{13}C NMR (125 MHz, chloroform-d_6) δ ppm: 168.63, 160.44, 153.85, 146.31, 136.38, 134.06, 131.69, 130.61, 130.05, 127.02, 125.79, 118.81, 113.36, 109.34, 53.74. HRMS: *m/z* for $C_{15}H_{11}ClN_2O_2S$ ([M + H]$^+$): 320.0215, found 320.0211.

4-Hydroxy-*N*-(6-methoxybenzo[*d*]thiazol-2-yl)benzamide (5i): White solid, yield 83%, m.p.: 167-168 ºC; ^{1}H NMR (500 MHz, chloroform-d_6) δ ppm: 10.83 (s, 1H), 8.17 (s, 1H), 7.74 (d, *J* = 8.7 Hz, 2H), 7.61 (d, *J* = 7.8 Hz, 1H), 7.51 (d, *J* = 2.1 Hz, 1H), 7.14 (dd, *J* = 7.6, 2.2 Hz, 1H), 6.97 (d, *J* = 8.7 Hz, 2H), 3.77 (s, 3H). ^{13}C NMR (125 MHz, chloroform-d_6) δ ppm: 166.09, 161.60, 160.15, 154.28, 144.42, 131.74, 130.25, 125.14, 119.49, 117.32, 113.83, 108.83, 55.63. HRMS: *m/z* for $C_{15}H_{12}N_2O_3S$ ([M + H]$^+$): 301.0651, found 301.0645.

3-Hydroxy-*N*-(6-methoxybenzo[*d*]thiazol-2-yl)benzamide (5j): White solid, yield 83%, m.p.: 171-172 ºC; ^{1}H NMR (500 MHz, chloroform-d_6) δ ppm: 10.98 (s, 1H), 8.26 (s, 1H), 7.59 (d, *J* = 7.8 Hz, 1H), 7.51 (d, *J* = 2.1 Hz, 1H), 7.48-7.42 (m, 1H), 7.24 (t, *J* = 8.2 Hz, 1H), 7.16 (t, *J* = 2.2 Hz, 1H), 6.99 (dd, *J* = 7.8, 2.1 Hz, 1H), 6.90 (dt, *J* = 8.5, 1.6 Hz, 1H), 3.85 (s, 3H). ^{13}C NMR (125 MHz, chloroform-d_6) δ ppm: 168.41, 160.66, 157.30, 154.28, 144.64, 134.27, 132.68, 128.91, 119.49, 118.54, 117.31, 113.47, 112.60, 108.83, 54.47. HRMS: *m/z* for $C_{15}H_{12}N_2O_3S$ ([M + H]$^+$): 301.0651, found 301.0645.

***N*-(6-Methoxybenzo[*d*]thiazol-2-yl)-4-nitrobenzamide (5k):** Pale yellow solid, yield 78%, m.p.: 220-221 ºC; ^{1}H NMR (500 MHz, chloroform-d_6) δ ppm: 11.03 (s, 1H), 8.26 (d, *J* = 8.6 Hz, 2H), 8.07 (d, *J* = 8.5 Hz, 2H), 7.64 (d, *J* = 7.8 Hz, 1H), 7.55 (d, *J* = 2.1 Hz, 1H), 7.13 (dd, *J* = 7.6, 2.2 Hz, 1H), 3.85 (s, 3H). ^{13}C NMR (125 MHz, chloroform-d_6) δ ppm: 165.37, 160.15, 154.28, 148.78, 144.86, 137.61, 131.69, 131.04, 124.71, 119.92, 114.27, 109.34, 55.19. HRMS: *m/z* for $C_{15}H_{11}N_3O_4S$ ([M + H]$^+$): 330.0496, found 330.0492.

***N*-(6-Methoxybenzo[*d*]thiazol-2-yl)-3-nitrobenzamide (5l):** Pale yellow solid, yield 81%, m.p.: 214-215 ºC; ^{1}H NMR (500 MHz, chloroform-d_6) δ ppm: 11.11 (s, 1H), 8.86 (t, *J* = 2.2 Hz, 1H), 8.45 (ddt, *J* = 25.1, 8.7, 1.4 Hz, 2H), 7.74 (t, *J* = 8.5 Hz, 1H), 7.62 (d, *J* = 7.8 Hz, 1H), 7.56 (d, *J* = 2.1 Hz, 1H), 7.12 (dd, *J* = 7.6, 2.2 Hz, 1H), 3.86 (s, 3H). ^{13}C NMR (125 MHz, chloroform-d_6) δ ppm: 168.00, 158.77, 153.85, 148.92, 144.64, 133.80, 133.14, 131.69, 130.38, 126.52, 124.20, 119.92, 114.05, 109.12, 54.25. HRMS: *m/z* for $C_{15}H_{11}N_3O_4S$ ([M + H]$^+$): 330.0498, found 330.0492.

4-Amino-*N*-(6-methoxybenzo[*d*]thiazol-2-yl)benzamide (5m): White solid, yield 79%, m.p.: 208-209 ºC; ^{1}H NMR (500 MHz, chloroform-d_6) δ ppm: 10.78 (s, 1H), 7.71 (d, *J* = 8.1 Hz, 2H), 7.55 (d, *J* = 7.8 Hz, 1H), 7.45 (d, *J* = 2.2 Hz, 1H), 7.01 (dd, *J* = 7.7, 2.2 Hz, 1H), 6.52 (d, *J* = 8.2 Hz, 2H), 4.63 (s, 2H), 3.74 (s, 3H). ^{13}C NMR (125 MHz, chloroform-$_6$) δ ppm: 165.59, 158.34, 153.85, 151.24, 144.42, 133.33, 132.39, 126.52, 120.65, 114.99, 114.48, 108.83, 55.63. HRMS: *m/z* for $C_{15}H_{13}N_3O_2S$ ([M + H]$^+$): 300.0784, found 300.0781.

4-((6-Methoxybenzo[*d*]thiazol-2-yl)carbamoyl)benzoic acid (5n): White solid, yield 73%, m.p.: 234-235 ºC; ^{1}H NMR (500 MHz, chloroform-d_6) δ ppm: 11.70 (s, 1H), 10.90 (s, 1H),

8.03-7.93 (m, 4H), 7.62 (d, *J* = 7.8 Hz, 1H), 7.55 (d, *J* = 2.1 Hz, 1H), 7.12 (dd, *J* = 7.6, 2.2 Hz, 1H), 3.89 (s, 3H). ^{13}C NMR (125 MHz, chloroform-d_6) δ ppm: 169.88, 168.63, 160.44, 154.28, 146.31, 136.88, 132.39, 131.40, 129.21, 128.44, 119.70, 114.99, 110.50, 55.19. HRMS: *m/z* for $C_{16}H_{12}N_2O_4S$ ([M + H]$^+$): 329.0611, found 329.0604.

MTT assay: An MTT assay was evaluated to assess the anticancer efficacy of benzothiazole hybrids (**5a-n**) on MCF-7 (breast cancer), HCT-116 (colon cancer) and HEK-293 (normal human embryonic kidney) cell lines. The cell lines were cultured in RPMI-1640 or DMEM media enriched with 10% fetal bovine serum (FBS) and 1% penicillin-streptomycin at 37 ºC in a humidified environment containing 5% CO_2. Upon achieving 70-80% confluence, adherent cells (MCF-7, HCT-116 and HEK-293) were subjected to trypsinization using trypsin-EDTA, whereas suspension cells were delicately disaggregated using pipetting. Approximately 5,000-10,000 cells per well were inoculated in 96-well plates containing 100 µL of complete media and permitted to adhere and stabilize for 24 h.

Serial dilutions of benzothiazole hybrids (**5a-n**) were prepared in complete medium, achieving concentrations ranging from 0.1 µM to 100 µM. The medium in each well was replaced with 100 µL of compound dilutions, while control wells received an equivalent volume of DMSO (vehicle control). After 48 h of incubation, 10 µL of MTT reagent (5 mg/mL in PBS) was added to each well and the plates were incubated for an additional 4 h at 37 ºC to allow for the formation of formazan crystals. Subsequently, the medium was carefully aspirated and 100 µL of DMSO was added to each well to dissolve the formazan crystals. The plates were gently agitated for 10-15 min to ensure complete dissolution. The absorbance was measured at 570 nm using a microplate reader, with a reference wavelength of 630 nm to correct for background absorbance. The IC_{50} values, representing the compound concentration required to inhibit cell growth by 50%, were determined by plotting cell viability against compound concentration. All experiments were conducted under sterile conditions to avoid contamination and each concentration was tested in triplicate (n = 3) to ensure data accuracy and reproducibility [29].

Molecular docking: The X-ray crystal structures of the EGFR kinase domain in complex with gefitinib (PDB: 4WKQ) and EGFR in complex with osimertinib (PDB: 6LUD) were provided by the Protein Data Bank. Hydrogen atoms were introduced and bond orders were assigned to the protein's 3D structure by the Protein Preparation Wizard feature in Schrödinger software. The OPLS 2005 force field was employed by the LigPrep module in Schrödinger software to optimize the 3D structures of chiral ligands. The SITEMAP Analysis Tool of Maestro 11.8 was employed to analyze receptor sites for 5E1E, 7RN6 and 7SJ3, which was subsequently followed by the grid construction tool of the Schrödinger suite. The SP glide score was determined by evaluating the binding interaction energy, van der Waals energy, electrostatic potential energy and strain energy during molecular docking using Glide's standard precision docking modes (Glide XP). The Schrödinger Maestro interface was employed to investigate the binding of ligands to the active sites of EGFR and CDK-4 [30].

RESULTS AND DISCUSSION

The benzothiazole carboxamide hybrids (**5a-n**) were successfully synthesized following the outlined procedures. The intermediate 6-hydroxy-2-aminobenzothiazole (**3**) was prepared *via* a condensation reaction between benzoquinone and thiourea in refluxing ethanol, using conc. HCl as a catalyst. The subsequent methylation of compound **3** in the presence of K_2CO_3 and CH_3I in DMF afforded 6-methoxybenzo[*d*]-thiazol-2-amine (**4**). The final step involved the coupling of substituted carboxylic acids with the synthesized amine intermediates to obtain the target hybrids **5a-n**. All the compounds were synthesized in good yields.

Molecular docking with EGFR targets 4WKQ and 6LUD: The docking study evaluates the interaction of benzothiazole hybrids (**5a-n**) with two target proteins, 4WKQ and 6LUD, to determine their binding affinities based on docking scores. The resulted docking scores are shown in Table-1. These compounds incorporate acetamide and benzamide functionalities with diverse substituents on the benzothiazole ring. The docking scores, with more negative values indicating stronger binding, provide insights into the impact of these substituents on the interactions.

TABLE-1
DOCKING SCORES OF BENZOTHIAZOLE HYBRIDS (**5a-n**)

Compound	R	4WKQ	6LUD
5a	-CH_3	-6.319	-5.621
5b	-CH_2-CH_3	-5.423	-5.854
5c	-CH_2-CH_2-CH_3	-5.809	-5.579
5d	-C_6H_5	-6.132	-5.479
5e	-(C_6H_4)-4-CH_3	-6.266	-5.432
5f	-(C_6H_4)-3-CH_3	-6.997	-5.569
5g	-(C_6H_4)-4-Cl	-5.968	-5.456
5h	-(C_6H_4)-3-Cl	-6.894	-5.641
5i	-(C_6H_4)-4-OH	-6.366	-6.433
5j	-(C_6H_4)-3-OH	-7.488	-6.093
5k	-(C_6H_4)-4-NO_2	-6.172	-5.606
5l	-(C_6H_4)-3-NO_2	-6.098	-5.479
5m	-(C_6H_4)-4-NH_2	-6.411	-6.015
5n	-(C_6H_4)-4-COOH	-6.246	-5.69
	Gefitinib	-5.767	–
	Osimeritinib	–	-7.698

For 4WKQ, the best-performing compound is **5j** (-(C_6H_4)-3-OH), (Fig. 1) with a docking score of -7.488, indicating the strongest binding among all hybrids. This is followed by **5f** (-(C_6H_4)-3-CH_3) and **5h** (-(C_6H_4)-3-Cl), with scores of -6.997 and -6.894, respectively (Fig. 1). These results suggest that substituents at the *meta* position on the phenyl ring, particularly electron-donating groups like hydroxyl (-OH) and electron-withdrawing groups like chlorine (-Cl), contribute significantly to binding affinity. Compounds such as **5i** (-(C_6H_4)-4-OH) and **5m** (-(C_6H_4)-4-NH_2) also show good binding with scores of -6.366 and -6.411, respectively, highlighting the favourable influence of *para*-positioned functional groups.

In case of 6LUD, compound **5i** (-(C_6H_4)-4-OH) emerges as the top binder, with a score of -6.433, followed closely by compounds **5j** (-(C_6H_4)-3-OH) at -6.093 and **5m** (-(C_6H_4)-4-

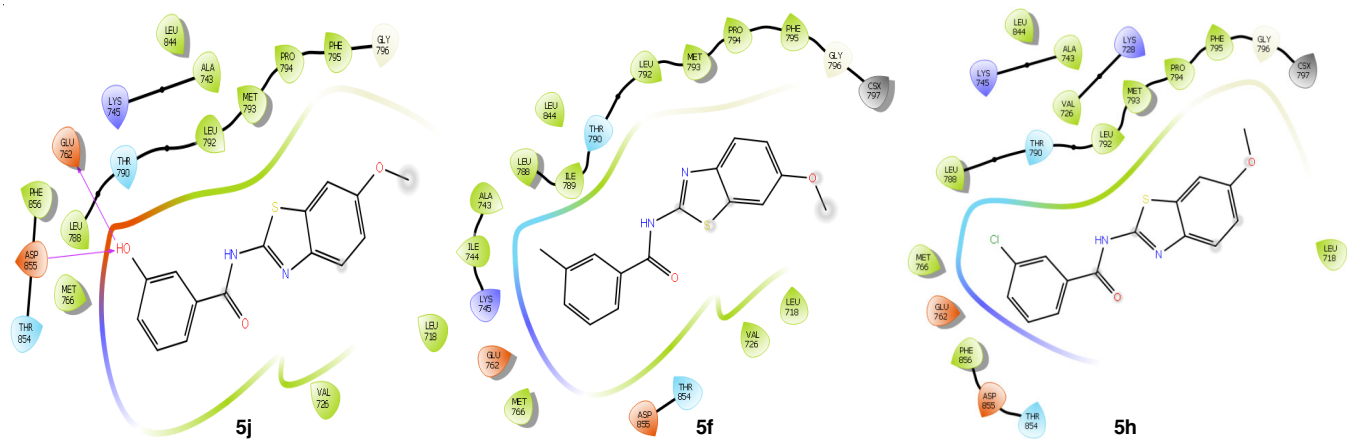

Fig. 1. Interactions of compounds **5j**, **5f** and **5h** at the active site of target 4WKQ

NH_2) at -6.015 (Fig. 2). These results suggest that the hydroxyl and amino groups enhance binding to this target as well. Halogen substituted derivatives, such as compound **5h** (-(C_6H_4)-3-Cl), exhibit moderate affinity with a docking score of -5.641, indicating a role for halogens in binding, though less pronounced compared to hydroxyl and amino groups.

Substituents on the phenyl ring significantly influence the binding affinities. Electron-donating groups like hydroxyl (-OH) and amino (-NH_2) enhance binding, as observed in compounds **5i**, **5j** and **5m**, likely due to their ability to form hydrogen bonds or electrostatic interactions with the target proteins. Halogenated compounds, such as compound **5h** (3-Cl), show variable effects, with good affinity for 4WKQ but slightly lower performance with 6LUD. In contrast, alkyl groups like those in compounds **5a** (-CH_3), **5b** (-CH_2-CH_3) and **5c** (-CH_2-CH_2-CH_3) are less effective, likely due to their inability to engage in strong intermolecular interactions with the binding sites.

When compared to reference drugs, gefitinib shows a docking score of -5.767 with 4WKQ, which is lower than many benzothiazole hybrids, including compounds **5j**, **5f** and **5h**, indicating the potential of the hybrids as effective binders for this target. However, osimertinib, with a score of -7.698 for 6LUD, surpasses all designed hybrids, demonstrating its superior binding affinity to this target. These findings suggest that while the benzothiazole hybrids are promising, further optimization is needed to achieve binding affinities comparable to benchmark drugs. The benzothiazole hybrids, particularly those with hydroxyl (-OH) and amino (-NH_2) substituents, exhibit strong binding to both 4WKQ and 6LUD, with compounds **5j** and **5i** standing out as the top candidates.

Anticancer activity: The IC_{50} values of the synthesized compounds **5a-n** against MCF-7 breast cancer cells, HCT-116 colon cancer cells and HEK-293 normal cells were evaluated using the MTT assay. Lower IC_{50} values indicate higher cytotoxic activity and the results were compared with doxorubicin, a standard chemotherapeutic agent (Table-2). The IC_{50} of doxorubicin (2.09 ± 0.75 µM) was significantly lower than all synthesized compounds, highlighting its superior potency. However, several derivatives, particularly compounds **5f**, **5h**, **5i**, **5j** and **5m**, showed promising activity.

Lung cancer cell lines (MCF-7): Among the synthesized compounds with aliphatic substituents, compound **5b** (-CH_2-CH_3) exhibited the highest activity (IC_{50} = 13.20 ± 1.82 µM), outperforming compounds **5a** (-CH_3) and **5c** (-CH_2-CH_2-CH_3). This trend suggests that increasing hydrophobicity enhances activity up to a certain limit, beyond which steric hindrance or reduced solubility may diminish efficacy. Compounds with the aromatic substituents displayed diverse activities influenced by the type and position of substituent. For example, **5f** (3-CH_3, IC_{50} = 6.23 ± 0.97 µM) demonstrated significantly higher

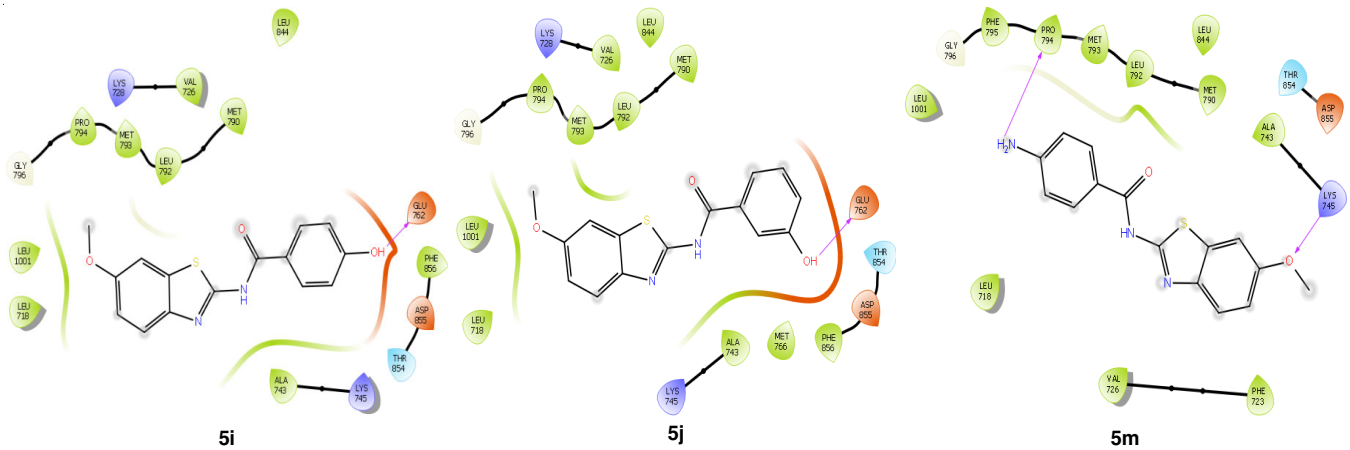

Fig. 2. Interactions of compounds **5i**, **5j** and **5m** at the active site of target 4WKQ

TABLE-2
IC_{50} VALUES OF THE SYNTHESIZED BENZOTHIAZOLE HYBRIDS (**5a-n**) FROM MTT ASSAY

Compound	IC_{50} values (μM)		
	MCF-7 (breast cancer)	HCT-116 (colon cancer)	HEK-293 (normal human embryonic kidney)
5a	19.08 ± 2.91	16.09 ± 0.91	33.30 ± 1.24
5b	13.20 ± 1.82	13.69 ± 0.92	31.04 ± 1.27
5c	15.82 ± 1.26	20.96 ± 1.23	29.47 ± 3.55
5d	17.65 ± 1.01	17.43 ± 0.97	28.02 ± 1.58
5e	17.62 ± 1.12	14.00 ± 1.59	30.80 ± 1.04
5f	6.23 ± 0.97	8.86 ± 1.44	28.56 ± 1.92
5g	16.09 ± 0.91	17.34 ± 1.47	28.35 ± 0.99
5h	7.99 ± 0.96	11.06 ± 1.50	30.39 ± 0.89
5i	7.18 ± 0.97	7.91 ± 1.44	24.21 ± 3.55
5j	6.51 ± 0.97	7.44 ± 1.77	33.55 ± 0.71
5k	19.84 ± 1.77	17.23 ± 2.06	29.81 ± 1.24
5l	20.35 ± 0.96	24.96 ± 1.44	33.55 ± 0.84
5m	6.11 ± 1.09	7.26 ± 1.03	23.72 ± 2.39
5n	12.06 ± 0.91	12.42 ± 1.28	26.61 ± 2.53
Doxorubicin	2.09±0.75	3.14±0.56	4.83±1.12

potency than **5e** (4-CH_3, IC_{50} = 17.62 ± 1.12 μM), indicating that the *meta* position enhances cytotoxicity, likely due to improved spatial orientation for interaction with the target.

Halogen-substituted derivatives also followed a similar pattern, with the *meta*-chloro derivative **5h** (IC_{50} = 7.99 ± 0.96 μM) being more potent than the *para*-chloro derivative **5g** (IC_{50} = 16.09 ± 0.91 μM). Hydroxy-substituted compounds, **5i** (4-OH) and **5j** (3-OH), showed IC_{50} values of 7.18 ± 0.97 μM and 6.51 ± 0.97 μM, respectively. Their high activity can be attributed to the ability of hydroxyl groups to form hydrogen bonds with the target, with the *meta* position again proving slightly more favourable. Conversely, nitro derivatives (**5k** and **5l**) exhibited the least activity (IC_{50} = 19.84 ± 1.77 and 20.35 ± 0.96 μM, respectively), potentially due to the bulky and strongly electron-withdrawing nature of the nitro group, which may interfere with effective binding. The amino-substituted compound **5m** (4-NH_2) emerged as one of the most potent derivatives (IC_{50} = 6.11 ± 1.09 μM), likely due to its electron-donating nature and the ability to form hydrogen bonds. In contrast, the carboxylic acid derivative **5n** (4-COOH) displayed moderate activity (IC_{50} = 12.06 ± 0.91 μM), possibly due to its acidic nature, which may affect cellular uptake or membrane permeability.

The structure-activity relationship (SAR) analysis revealed that the substituent position, hydrophobicity and the ability to form hydrogen bonds significantly impact cytotoxic activity. The *meta*-substituted derivatives consistently outperformed their *para*-substituted counterparts and electron-donating groups (*e.g.* -CH_3, -NH_2) were generally more favourable than electron withdrawing groups (*e.g.* -NO_2). Compounds **5f**, **5h**, **5i**, **5j** and **5m** exhibited the most promising IC_{50} values, suggesting their potential as lead candidates for further optimization and development in breast cancer therapy.

Against colon cancer cell lines (HCT-116): Among the tested compounds several derivatives, compounds **5f**, **5h**, **5i**, **5j** and **5m**, demonstrated promising cytotoxic activity, with IC_{50} values below 10 μM. Among aliphatic-substituted derivatives, **5b** (-CH_2-CH_3) showed the best activity (IC_{50} = 13.69 ± 0.92 μM), outperforming **5a** (-CH_3) and **5c** (-CH_2-CH_2-CH_3). The trend suggests that moderate chain length enhances activity, while larger substituents like -CH_2-CH_2-CH_3 in **5c** (IC_{50} = 20.96 ± 1.23 μM) might introduce steric hindrance or affect cellular uptake. Aromatic derivatives showed variations based on the type and position of substituents. For example, compound **5f** (3-CH_3) displayed significantly higher potency (IC_{50} = 8.86 ± 1.44 μM) compared to compound **5e** (4-CH_3, IC_{50} = 14.00 ± 1.59 μM), indicating a preference for the *meta* position.

Halogen-substituted derivatives also exhibited position-dependent activity, with compound **5h** (3-Cl, IC_{50} = 11.06 ± 1.50 μM) showing better activity than **5g** (4-Cl, IC_{50} = 17.34 ± 1.47 μM). Hydroxy-substituted compounds, **5i** (4-OH) and **5j** (3-OH), were among the most potent, with IC_{50} values of 7.91 ± 1.44 and 7.44 ± 1.77 μM, respectively. This high activity is likely attributed to the ability of hydroxyl groups to form hydrogen bonds, facilitating strong interactions with the target. The *meta* position again slightly outperformed the *para* position, as observed in other substituent groups.

In contrast, nitro-substituted derivatives **5k** (4-NO_2, IC_{50} = 17.23 ± 2.06 μM) and **5l** (3-NO_2, IC_{50} = 24.96 ± 1.44 μM) showed the least activity, likely due to the bulky and electron withdrawing nature of nitro group, which may disrupt favourable interactions with the biological target. Interestingly, compound **5m** (4-NH_2) emerged as one of the most active compounds (IC_{50} = 7.26 ± 1.03 μM), highlighting the significance of electron-donating substituents and their ability to form hydrogen bonds. Similarly, compound **5n** (4-COOH, IC_{50} = 12.42 ± 1.28 μM) exhibited moderate activity, possibly due to its acidic nature, which could impact cellular uptake.

The structure-activity relationship (SAR) analysis suggested that the cytotoxic activity of these compounds is influenced by the type and position of substituents. The *meta*-substituted derivatives generally outperformed their *para*-substituted counterparts and electron-donating groups (*e.g.* -CH_3, -NH_2, -OH) enhanced activity compared to electron-withdrawing groups (*e.g.* -NO_2). Compounds **5f**, **5h**, **5i**, **5j** and **5m** showed the most promising results and could serve as lead molecules for further optimization in colon cancer therapy.

The cytotoxicity of the synthesized compounds **5a-n** was evaluated against normal human embryonic kidney (HEK-293) cells to assess their selectivity and potential toxicity to normal cells. The synthesized compounds displayed significantly reduced cytotoxicity toward normal HEK-293 cells compared to the two cancer cell lines tested, suggesting their potential for selective anticancer activity. Among the derivatives, compounds **5m** (4-NH_2) and **5i** (4-OH) exhibited relatively higher toxicity to normal cells, indicating the need for careful consideration of their therapeutic window.

The correlation between the anticancer activity of the synthesized benzothiazole hybrids (**5a-n**) and their docking scores for the 4WKQ and 6LUD protein targets provides valuable insights into their structure-activity relationships (SAR). By analyzing the IC_{50} values for MCF-7 (breast cancer), HCT-116 (colon cancer) and HEK-293 (normal human embryonic kidney) cells in relation to docking scores, the predictive

power of molecular docking for biological activity can be assessed.

For instance, in MCF-7 breast cancer cell line, compounds with lower docking scores (more negative values) against the 4WKQ protein demonstrated enhanced anticancer activity, as reflected by lower IC_{50} values. Compound **5f** with a docking score of -6.997 exhibited potent activity (IC_{50} = 6.23 ± 0.97 µM) and **5j** (-7.488) showed similar potency (IC_{50} = 6.51 ± 0.97 µM). In contrast, compound **5b** with a higher docking score (-5.423) displayed reduced potency (IC_{50} = 13.20 ± 1.82 µM). This suggests a strong correlation between docking scores and biological activity, particularly for interactions with 4WKQ. A similar trend was observed for the HCT-116 colon cancer cell line. For example, compounds with lower docking scores against 4WKQ and 6LUD generally exhibited greater anticancer activity. For instance, compound **5m** (-6.411, -6.015) showed high potency (IC_{50} = 7.26 ± 1.03 µM), aligning with its favourable docking scores. Similarly, compound **5i** (-6.366, -6.433) demonstrated excellent activity (IC_{50} = 7.91 ± 1.44 µM). However, some exceptions were also observed, for example, **5h** compound (-6.894) displayed strong activity (IC_{50} = 11.06 ± 1.50 µM) despite slightly less favourable docking scores compared to compound **5i**. This variation may result from molecular interactions not fully captured by docking simulations.

The SAR analysis revealed that compounds with specific substitutions, such as hydroxyl (-OH), amino (-NH_2) and *meta*-methyl (-CH_3) groups, consistently exhibited strong anticancer activity with favourable selectivity. Compounds **5f**, **5i**, **5j** and **5m** were particularly effective against cancer cells while sparing normal cells, consistent with their lower docking scores and high binding affinity to target proteins.

Conclusion

The synthesized benzothiazole carboxamide hybrids (**5a-n**) exhibited promising binding affinities and anticancer activities, particularly against MCF-7 and HCT-116 cancer cell lines. Molecular docking studies revealed that the presence of hydroxyl and amino substituents enhanced the binding interactions with EGFR targets 4WKQ and 6LUD. The structure-activity relationship (SAR) analysis demonstrated that the position of substituents, along with their electron-donating or withdrawing properties, plays a crucial role in determining the anticancer activity. The compounds showed reduced cytotoxicity towards normal HEK-293 cells, suggesting their potential for selective anticancer action. Overall, the results highlight the therapeutic potential of these hybrids, particularly compounds **5f**, **5h**, **5i**, **5j** and **5m**, as promising candidates for further optimization and development in cancer therapy.

ACKNOWLEDGEMENTS

The support provided by the Andhra University and Sir C R Reddy College of Pharmaceutical Sciences is gratefully acknowledged.

CONFLICT OF INTEREST

The authors declare that there is no conflict of interests regarding the publication of this article.

REFERENCES

1. GBD 2021 Forecasting Collaborators, *Lancet*, **403**, 2204 (2024); https://doi.org/10.1016/S0140-6736(24)00685-8
2. P. Piña-Sánchez, A. Chávez-González, M. Ruiz-Tachiquín, E. Vadillo, A. Monroy-García, J.J. Montesinos, R. Grajales, M. Gutiérrez de la Barrera and H. Mayani, *Cancer Contr.*, **28**, 10732748211038735 (2021); https://doi.org/10.1177/10732748211038735
3. C.S. Pramesh, R.A. Badwe, N. Bhoo-Pathy, G. Chinnaswamy, A.J. Dare, C.M. Booth, V.P. De Andrade, D.J. Hunter, M. Gospodarowicz, S. Gopal, S. Gunasekera, A. Ilbawi, S. Kapambwe, P. Kingham, T. Kutluk, N. Lamichhane, M. Mutebi, J. Orem, G. Parham, P. Ranganathan, M. Sengar, R. Sullivan, S. Swaminathan, I.F. Tannock, V. Tomar, V. Vanderpuye, C. Varghese and E. Weiderpass, *Nat. Med.*, **28**, 649 (2022); https://doi.org/10.1038/s41591-022-01738-x
4. M. Puyol, J. Seoane, E. Aguilar, L.B. Vozza, I. Orbe, K.H. Crawford, A. Fernández, F. Bray, S.E. Johnson and S. Gopal, *Clin. Cancer Res.*, **27**, 963 (2021); https://doi.org/10.1158/1078-0432.CCR-20-2978
5. L.V. Zhilitskaya, B.A. Shainyan and N.O. Yarosh, *Molecules*, **26**, 2190 (2021); https://doi.org/10.3390/molecules26082190
6. X. Gao, J. Liu, X. Zuo, X. Feng and Y. Gao, *Molecules*, **25**, 1675 (2020); https://doi.org/10.3390/molecules25071675
7. K.P. Yadav, M.A. Rahman, S. Nishad, S.K. Maurya, M. Anas and M. Mujahid, *Intelligent Pharm.*, **1**, 122 (2023); https://doi.org/10.1016/j.ipha.2023.06.001
8. K. Haider, N. Shrivastava, A. Pathak, R.P. Dewangan, S. Yahya and M.S. Yar, *Results Chem.*, **4**, 100258 (2022); https://doi.org/10.1016/j.rechem.2021.100258
9. M. Videnoviæ, M. Mojsin, M. Stevanoviæ, I. Opsenica, T. Srdiæ-Rajiæ and B. Šolaja, *Eur. J. Med. Chem.*, **157**, 1096 (2018); https://doi.org/10.1016/j.ejmech.2018.08.067
10. F. Corbo, A. Carocci, D. Armenise, N. De Laurentis, A. Laghezza, F. Loiodice, P. Ancona, M. Muraglia, V. Pagliarulo, C. Franchini and A. Catalano, *J. Chem.*, **2016**, 4267564 (2016); https://doi.org/10.1155/2016/4267564
11. M.R. Aouad, M.A. Almehmadi, N. Rezki, F.F. Al-Blewi, M. Messali and I. Ali, *J. Mol. Struct.*, **1188**, 153 (2019); https://doi.org/10.1016/j.molstruc.2019.04.005
12. R. Fekri, M. Salehi, A. Asadi and M. Kubicki, *Inorg. Chim. Acta*, **484**, 245 (2019); https://doi.org/10.1016/j.ica.2018.09.022
13. A. Modi, M. Singh, G. Gutti, O.R. Shanker, V.K. Singh, S. Singh, S.K. Singh, S. Pradhan and G. Narayan, *Invest. New Drugs*, **38**, 934 (2020); https://doi.org/10.1007/s10637-019-00848-7
14. S. Harisha, J. Keshavayya, S.M. Prasanna and H. Joy Hoskeri, *J. Mol. Struct.*, **1218**, 128477 (2020); https://doi.org/10.1016/j.molstruc.2020.128477
15. L. Racané, L. Ptièek, G. Fajdetiæ, V. Tralic-Kulenovic, M. Klobuèar, S. Kraljevic-Pavelic, M. Peric, H.È. Paljetak, D. Verbanac and K. Starševic, *Bioorg. Chem.*, **95**, 103537 (2020); https://doi.org/10.1016/j.bioorg.2019.103537
16. A.M.S. Hebishy, M.S. Abdelfattah, A. Elmorsy and A.H.M. Elwahy, *J. Heterocycl. Chem.*, **57**, 2256 (2020); https://doi.org/10.1002/jhet.3947
17. S. Narva, S. Chitti, S. Amaroju, S. Goud, M. Alvala, D. Bhattacharjee, N. Jain and C.S.K.V. Gowri, *J. Heterocycl. Chem.*, **56**, 520 (2019); https://doi.org/10.1002/jhet.3427
18. J. Song, Q.L. Gao, B.W. Wu, T. Zhu, X.X. Cui, C.J. Jin, S.Y. Wang, S.H. Wang, D.J. Fu, H.M. Liu, S.Y. Zhang, Y.B. Zhang and Y.C. Li, *Eur. J. Med. Chem.*, **203**, 112618 (2020); https://doi.org/10.1016/j.ejmech.2020.112618
19. N. Rezki, M.A. Almehmadi, S. Ihmaid, A.M. Shehata, A.M. Omar, H.E.A. Ahmed and M.R. Aouad, *Bioorg. Chem.*, **103**, 104133 (2020); https://doi.org/10.1016/j.bioorg.2020.104133
20. D. Osmaniye, S. Levent, A.B. Karaduman, S. Ilgýn, Y. Özkay and Z.A. Kaplancikli, *Molecules*, **23**, 1054 (2018); https://doi.org/10.3390/molecules23051054

21. D. Yip, M.N. Le, J.L. Chan, J.H. Lee, J.A. Mehnert, A. Yudd, J. Kempf, W.J. Shih, S. Chen and J.S. Goydos, *Clin. Cancer Res.*, **15**, 3896 (2009); https://doi.org/10.1158/1078-0432.CCR-08-3303
22. Q. Xu, C. Liu, J. Zang, S. Gao, C.J. Chou and Y. Zhang, *Front. Cell Dev. Biol.*, **8**, 454 (2020); https://doi.org/10.3389/fcell.2020.00454
23. E.A. El-Meguid, G.O. Moustafa, H.M. Awad, E.R. Zaki and N.S. Nossier, *J. Mol. Struct.*, **1240**, 130595 (2021); https://doi.org/10.1016/j.molstruc.2021.130595
24. E.A. Abd El-Meguid, A.M. Naglah, G.O. Moustafa, H.M. Awad and A.M. El Kerdawy, *Bioorg. Med. Chem. Lett.*, **58**, 128529 (2022); https://doi.org/10.1016/j.bmcl.2022.128529
25. M.M. Al-Sanea, A. Hamdi, A.A.B. Mohamed, H.W. El-Shafey, M. Moustafa, A.A. Elgazar, W.M. Eldehna, H. Ur Rahman, D.G.T. Parambi, R.M. Elbargisy, S. Selim, S.N.A. Bukhari, O. Magdy Hendawy and S.S. Tawfik, *J. Enzyme Inhib. Med. Chem.*, **38**, 2166036 (2023); https://doi.org/10.1080/14756366.2023.2166036
26. W.A. Ewes, S.S. Tawfik, A.M. Almatary, M. Ahmad Bhat, H.W. El-Shafey, A.A.B. Mohamed, A. Haikal, M.A. El-Magd, A.A. Elgazar, M. Balaha and A. Hamdi, *Molecules*, **29**, 3186 (2024); https://doi.org/10.3390/molecules29133186
27. P. Linciano, C. Pozzi, L.D. Iacono, F. Di Pisa, G. Landi, A. Bonucci, S. Gul, M. Kuzikov, B. Ellinger, G. Witt, N. Santarem, C. Baptista, C. Franco, C.B. Moraes, W. Müller, U. Wittig, R. Luciani, A. Sesenna, A. Quotadamo, S. Ferrari, I. Pöhner, A. Cordeiro-da-Silva, S. Mangani, L. Costantino and M.P. Costi, *J. Med. Chem.*, **62**, 3989 (2019); https://doi.org/10.1021/acs.jmedchem.8b02021
28. N. Fattahi, M. Ayubi and A. Ramazani, *Tetrahedron*, **74**, 4351 (2018); https://doi.org/10.1016/j.tet.2018.06.064
29. P. Kumar, A. Nagarajan and P.D. Uchil, *Cold Spring Harb. Protoc.*, **2018**, pdb-rot095505 (2018); https://doi.org/10.1101/pdb.prot095505
30. J. Jiménez-Luna, A. Cuzzolin, G. Bolcato, M. Sturlese and S. Moro, *Molecules*, **25**, 2487 (2020); https://doi.org/10.3390/molecules25112487